Paleoceanography and Paleoclimatology

Supporting Information for

Paleoclimate Changes in the Pacific Northwest Over the Past 36,000 Years from Clumped Isotope Measurements and Model Analysis

Ricardo Lopez-Maldonado[1,2], Jesse Bloom Bateman[2,3], Andre Ellis[1], Nicholas E. Bader[4], Pedro Ramirez[1], Alexandrea Arnold[2], Osinachi Ajoku[5,6], Hung-I Lee[2,7], Gregory Jesmok[2,8], Deepshikha Upadhyay[2], Bryce Mitsunaga[2,9], Ben Elliott[2], Clay Tabor[10], and Aradhna Tripati[2,11]

[1]*Department of Geoscience and Environment, California State University, Los Angeles, CA, U.S.A.*

[2]*Department of Atmospheric and Oceanic Sciences, Department of Earth, Planetary, and Space Sciences, Institute of the Environment and Sustainability, Center for Diverse Leadership in Science, American Indian Studies Center, University of California, Los Angeles, CA, U.S.A.*

[3]*Department of Biology, SUNY Cortland, Cortland, NY, U.S.A.*

[4]*Department of Geology, Whitman College, Walla Walla, WA, U.S.A.*

[5]*Department of Interdisciplinary Studies, Howard University, Washington DC, USA*

[6]*National Center for Atmospheric Research, Boulder, COA, U.S.A.*

[7]*Department of Geophysical Sciences, University of Chicago, Chicago, IL, U.S.A.*

[8]*Department of Geology, California State University, Northridge, CA, U.S.A.*

[9]*Department of Geology, Brown University, Providence, RI, U.S.A.*

[10]*Department of Geosciences, University of Connecticut, Storrs, CT, U.S.A.*

[11]*UMR6538 Géosciences Océan, Institut Universitaire Européen de la Mer, Technopôle Brest-Iroise, Plouzané, 29280, France*

Contents of this file

Text S1
Figures S1 to S8
Tables S1 to S7

Additional Supporting Information (Files uploaded separately)

Captions for Tables S1 to S7

Introduction

We provide supporting information including a discussion of the materials and methods and analysis of results, six supporting figures, and seven supporting tables.

Text S1.

A. Materials and Methods

A1. Microscale pedogenic carbonate

For this study, we analyzed microscale pedogenic carbonates from the rhizosphere (Barta, 2011), specifically hypocoatings, which are thought to form on the order of weeks to months (Zamanian et al., 2016). Other microscale pedogenic carbonates that we identified in our samples and at our sites were carbonate coatings and calcite laminar caps (i.e. petrocalcic horizons). We did not use either the carbonate coatings or the calcite laminar caps in our analyses because these carbonates are believed to form on the order of 10^2 to 10^3 y. In the Sand Hills Coulee samples, we only found hypocoatings, whereas in the Washtucna paleosol we found both hypocoatings and carbonate coatings and observed a calcite laminar cap in the soil profile. Additional details are in the M.S. thesis of the lead author (Lopez-Maldonado, 2017).

A2. Detrital and pedogenic carbonate discrimination

We used two approaches to identify and differentiate between pedogenic carbonates and detrital carbonate in our samples to ensure that our results reflect the environment at the time of formation (pedogenic carbonates) and not subsequent alteration (detrital carbonates). First, we analyzed the Manganese:Calcium (Mn:Ca) and Magnesium:Calcium (Mg:Ca) ratios of samples to determine the purity of secondary carbonates (Li et al., 2013). Next, we examined the samples' micromorphology using thin sections of horizon samples. Both analyses were performed at California State University, Los Angeles (Cal State LA).

To analyze the samples Mn:Ca and Mg:Ca ratios, we digested samples in 0.2 M acetic acid for 24 h. After digestion we centrifuged the samples, and then collected the supernatant for analysis on a Perkin-Elmer ICP-OES Optima 5300. A calibrated blank and a 5 M Sigma-Aldrich multi-element standard solution were run to verify the accuracy and precision of the analysis. Analytical standard errors were <5%.

To analyze micromorphology, we sent samples to Quality Thin Sections (Tucson, AZ) for thin section preparation. Quality Thin Sections impregnated disturbed samples with epoxy, cut them into thin sections, and stained the thin sections with alizarin red-S and potassium ferricyanide. After thin section preparation, we analyzed the samples using standard petrographic microscope techniques.

A3. Stable isotope analysis

Initial sample preparation was carried out at California State University, Los Angeles (Cal State LA) in the environmental geochemistry laboratory. The samples were crushed by an agate mortar and pestle that was wiped down with 10% HCL, rinsed with deionized water (NANOpure), and wiped dry with kimwipes between samples. Samples were then placed in a clean petri dish and soaked in 3% H2O2 for 4 hours to oxidize organics (Eagle et al., 2013). The residual liquid was then removed with a pipette and the samples were then rinsed 3 times with NANOpure water before placing damp samples to dry in an oven set at ~ 40 ºC. Individual petri dishes containing dried samples were then wrapped with parafilm and stored in a desiccator with silica gel desiccant to prevent isotopic exchange with ambient water vapor. Samples were individually homogenized at the University of California, Los Angeles (UCLA) in the microscopy laboratory with an agate mortar and pestle that was wiped down clean with 10% HCl and then wiped down with ethanol between samples.

In practice, clumped-isotope analysis requires CO_2 produced from phosphoric acid digestion of carbonate material to measure the abundance of ^{13}C-^{18}O bonds (Upadhyay et al., 2021). Samples are weighed out to contain approximately 5 mg of carbonate per silver capsule before analysis on a modified MAT 253 gas-source IRMS mass spectrometer used to measure carbonate molecular ion beams corresponding to M/Z 44 ($^{12}C^{16}O_2^+$), 45 ($^{13}C^{16}O_2^+$ and $^{12}C^{16}O^{17}O^+$), 46 ($^{12}C^{18}O^{16}O^+$, $^{13}C^{16}O^{17}O^+$, and $^{12}C^{17}O_2^+$), 47 ($^{13}C^{18}O^{16}O^+$, $^{12}C^{18}O^{17}O^+$, and $^{13}C^{17}O_2^+$), 48 ($^{12}C^{18}O_2^+$ and $^{13}C^{17}O^{18}O^+$), and 49 ($^{13}C^{18}O_2^+$) (Eiler, 2011).

All stable and clumped isotope analyses were performed in the Tripati lab at UCLA. Methodology used for analysis is described in detail in Upadhyay et al. (2021). 5 mg of carbonate per sample was run on either a Nu Perspective IS mass spectrometer or a Thermo Finnigan MAT 253 gas source mass spectrometer, respectively. To obtain pure CO_2 gas for analysis, the homogenized samples first go through an automated sampling process comprised of a Costech Zero Blank Autosampler and common acid bath coupled with a gas purification system and gas chromatograph (either from Thermo or Agilent). Acid temperature is kept at 90 ± 2 °C and is checked daily whilst the machine is in operation. The gas purification system uses a series of cryotraps to remove water vapor from the gas released upon reaction with the acid and a silver wool filter to remove SO_4^- compounds. Samples are then automatically transferred to the mass spectrometer for analysis. Both instruments were specially configured to make precise clumped isotope measurements of mass-47 CO_2. Values are measured against a high-purity working gas Oztech brand CO_2 reference gas (i.e. $\delta^{13}C$ = -3.60‰ V-PDB and $\delta^{18}O$ = 25.03‰ V-SMOW). Every sample run also included carbonate standards of known isotopic compositions that were analyzed between every 2-3 samples. Between 3 and 12 replicates were run of each sample, unless insufficient material limited sample analysis.

A4. Calculations to derive stable isotope values and their errors

The raw analyzed data collected must then be refined with a correctional procedure because clumped isotope analysis involves fragmentation and recombination reactions in ion sources and other analytical artifacts when obtaining Δ_{47} values. Dennis et al. (2011) empirically accounts for such fragmentation and recombination reactions in ion sources and other analytical artifacts. The approach to clumped isotope data analysis in Dennis et al. (2011) utilizes an empirical transfer function to convert data to a common absolute reference frame (ARF), which accounts for interlaboratory differences in mass spectrometers. The ARF is based on the

theoretical temperature dependence of equilibrium clumping in CO_2 described in Wang et al. (2004).

All data presented in this study are reported on the absolute reference frame (Dennis et al., 2011), with equilibrated gases and carbonate standards analyzed daily. All corrections and calculations were done in Easotope (John and Bowen, 2016). Both carbonate and gas standards are used to account for the non-linearity inside the mass spectrometer. Gas standards included were equilibrated at 25 or 1000 ºC and carbonate standards precipitated at 600 ºC (ETH 1 and 2; Bernasconi et al., 2021) were included in this correction. Each pair of standards with the same formation temperature had differing bulk isotopic compositions, with one endmember being isotopically depleted, and the other being relatively enriched in comparison. Following the non-linearity correction, the ETH suite and a suite of in-house carbonate standards were used to project measurements into the ICDES reference frame (Bernasconi et al., 2021).

A5. iCESM simulations

We performed three simulations with the isotope-enabled version of the Community Earth System Model version 1.2 (CESM1.2): 1) A preindustrial control (PI) experiment, 2) a LGM experiment with period appropriate boundary conditions, and 3) a LGM land-ice only (LGM-ice_only) experiment, using the LGM ice sheet configuration with PI CO_2 and orbital conditions.

Isotopes of oxygen and hydrogen are included in the dynamically coupled atmosphere (CAM5), ocean (POP2), land (CLM4), sea ice (CICE4), and river runoff (RTM) components. For this work, the atmosphere and land were run on a 1.9° latitude x 2.5° longitude finite-volume grid, and the ocean and sea ice used a ~1° rotated pole grid. Previous studies have shown that the simulated isotopic distributions compare favorably with observations and other models of similar complexity (Nusbaumer et al., 2017; Wong et al., 2017; Zhang et al., 2017; Zhu et al., 2017). Initial ocean oxygen isotopic distributions were taken from the GISS interpolated ocean $\delta^{18}O$ dataset (LeGrande and Schmidt, 2006). Ocean average $\delta^{18}O$ was increased by +1 ‰ for the LGM and LGM-ice only experiments, to account for the large ice sheets (Duplessy et al. 2002). Ice volume and topography came from the ICE-6G dataset (Peltier et al., 2015). All simulations were initialized from previous experiments and run for an additional 550 years with water isotope tracers, allowing the atmosphere, land, and upper ocean to reach near equilibrium; analyses were performed on the final 48 years of each simulation.

B. Analysis of Results

B1. Analysis of Mg/Ca and Mn/Ca ratios

Pure pedogenic carbonates are characterized by low Mg/Ca and Mn/Ca ratios. Mg/Ca and Mn/Ca in the carbonates from our samples ranged from 0.02 to 0.06 mol/mol and 0.03 to 0.15 mmol/mol, respectively (Figure S1-S2). Table S1 shows a summary of the Mg/Ca and Mn/Ca ratio data.

B2. Analysis of Micromorphology

The thin sections in plane-polarized light mainly show a pale structureless pink stain and a pseudofabric in the groundmass formed from non-calcareous silt (Figures S3. C, D, and Figure S4. A, E, and F). Dickson (1966) states that the pale pink stain covering the entire thin section results from the “floods” of carbon dioxide bubbles during the carbonate staining and indicates that calcite is the only carbonate mineral present. The structureless appearance and pseudofabric suggest a micritic and microsparite carbonate groundmass, which coincides with the dominant

pedogenic calcite form in the region (Busacca, 1989; Durand et al., 2010; McDonald and Busacca, 1992). Dissolution voids are not present, and re-precipitated carbonate cannot be distinguished in any of the thin sections.

Thin sections reveal that detrital carbonate grains exist in some of the horizons characterized as pure pedogenic carbonate by the Mg/Ca and Mn/Ca ratios in trace amounts. Under cross-polarized light the Sand Hills Coulee paleosol thin sections—excluding the WA-3 calcic horizon—produced second and third order reds, blues, and yellows (Figure S5). These colors are the result of the etching process and are indicative of the presence of detrital limestone or marble grains (Dickson, 1966). Visual inspection of the Washtucna paleosol thin sections in cross-polarized light also showed evidence of very few detrital carbonate grains (Figure S6. A, B, and D), and pedogenic carbonate coatings, which represent carbonate recrystallization, within and around mineral grains in the KP-1 cambic horizon (Figure S6. D).

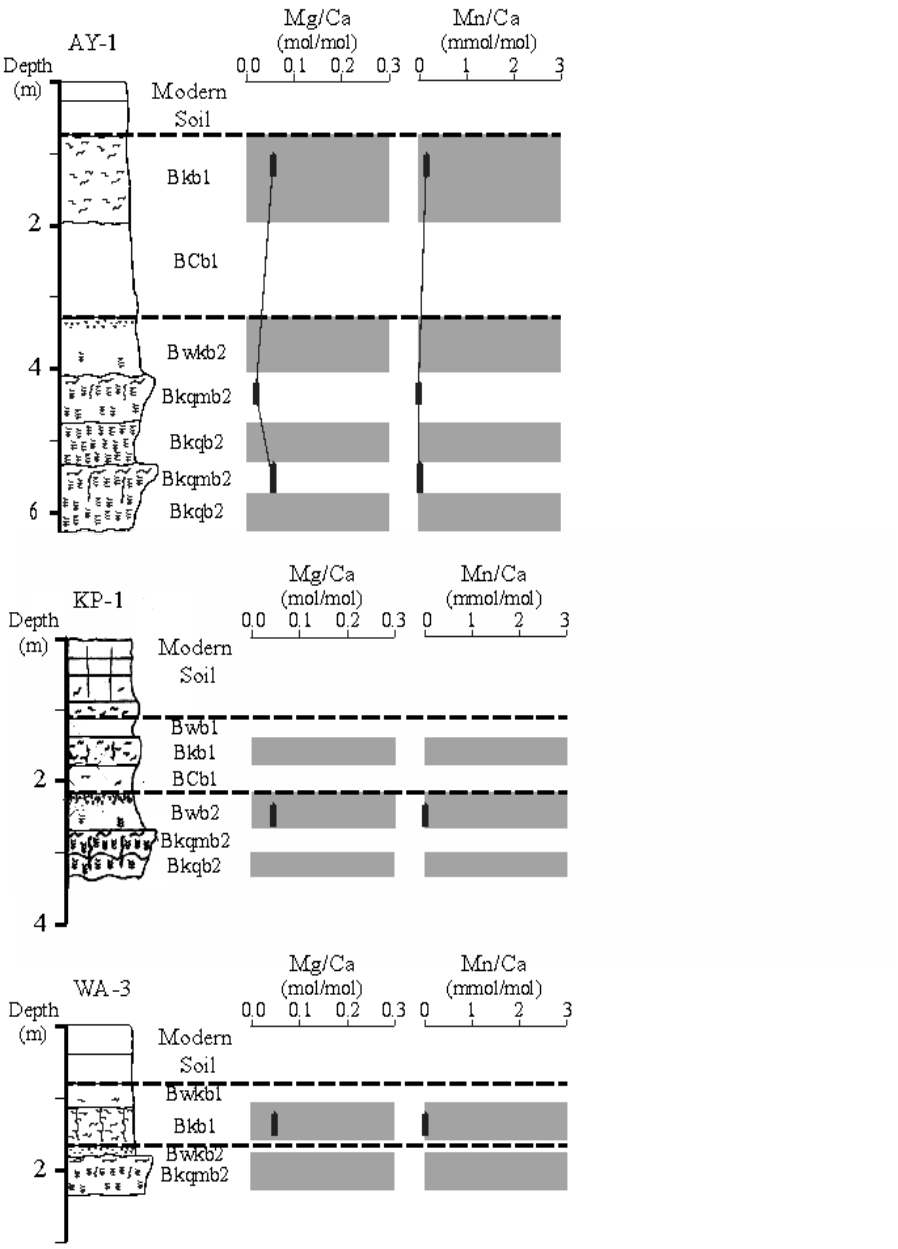

Figure S1. Mg/Ca and Mn/Ca ratios at AY-1, KP-1, and WA-3.

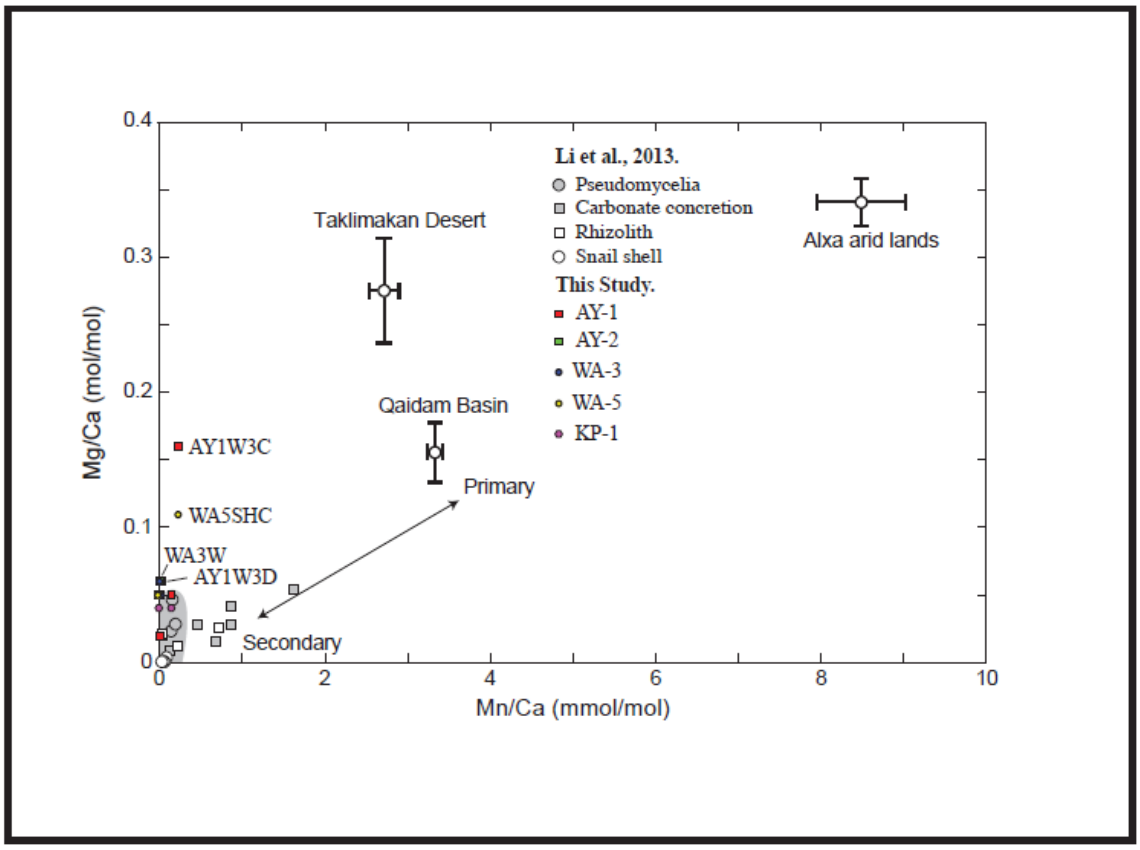

Figure S2. Mg/Ca and Mn/Ca ratios of pedogenic carbonates (modified from Li et al., 2013).

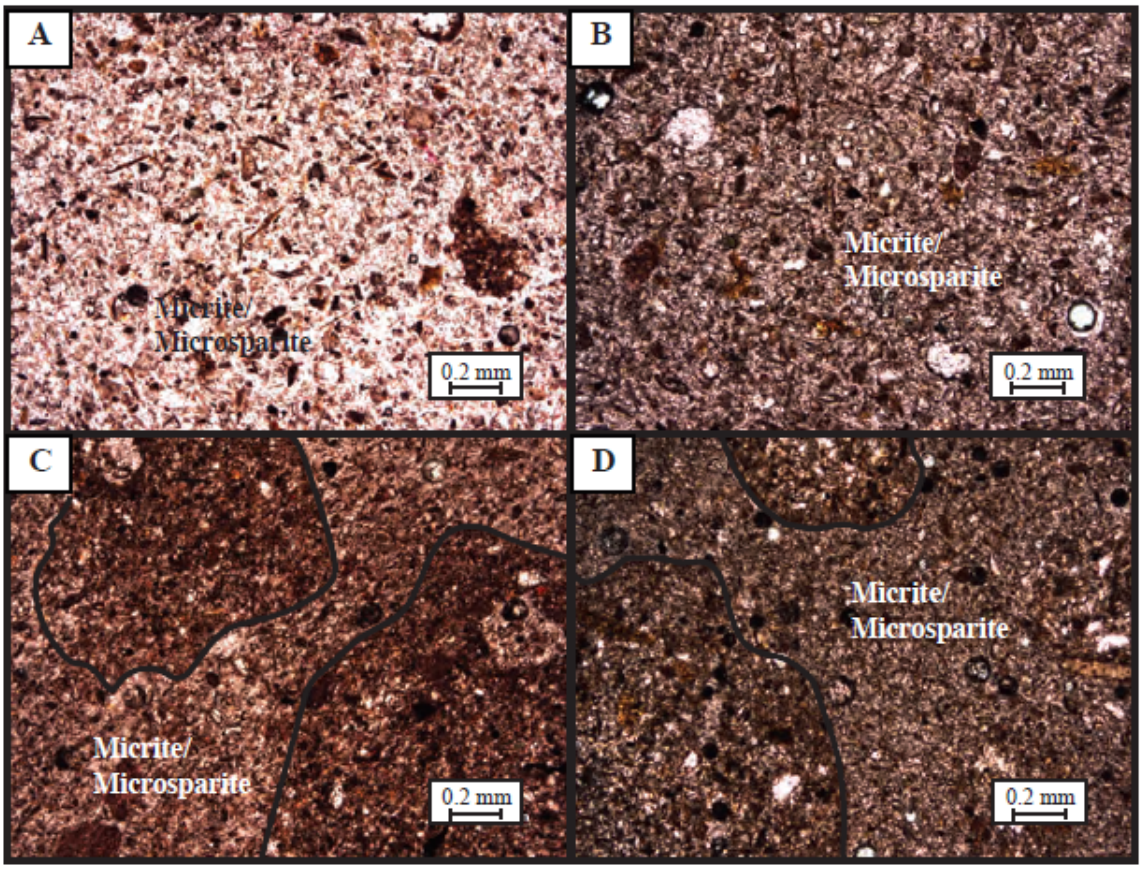

Figure S3. Examples of Sand Hills Coulee paleosol thin sections in plane polarized light. Thin sections are carbonate stained with alizarin red-s and potassium ferricynide, and depict the entire area containing micrite.

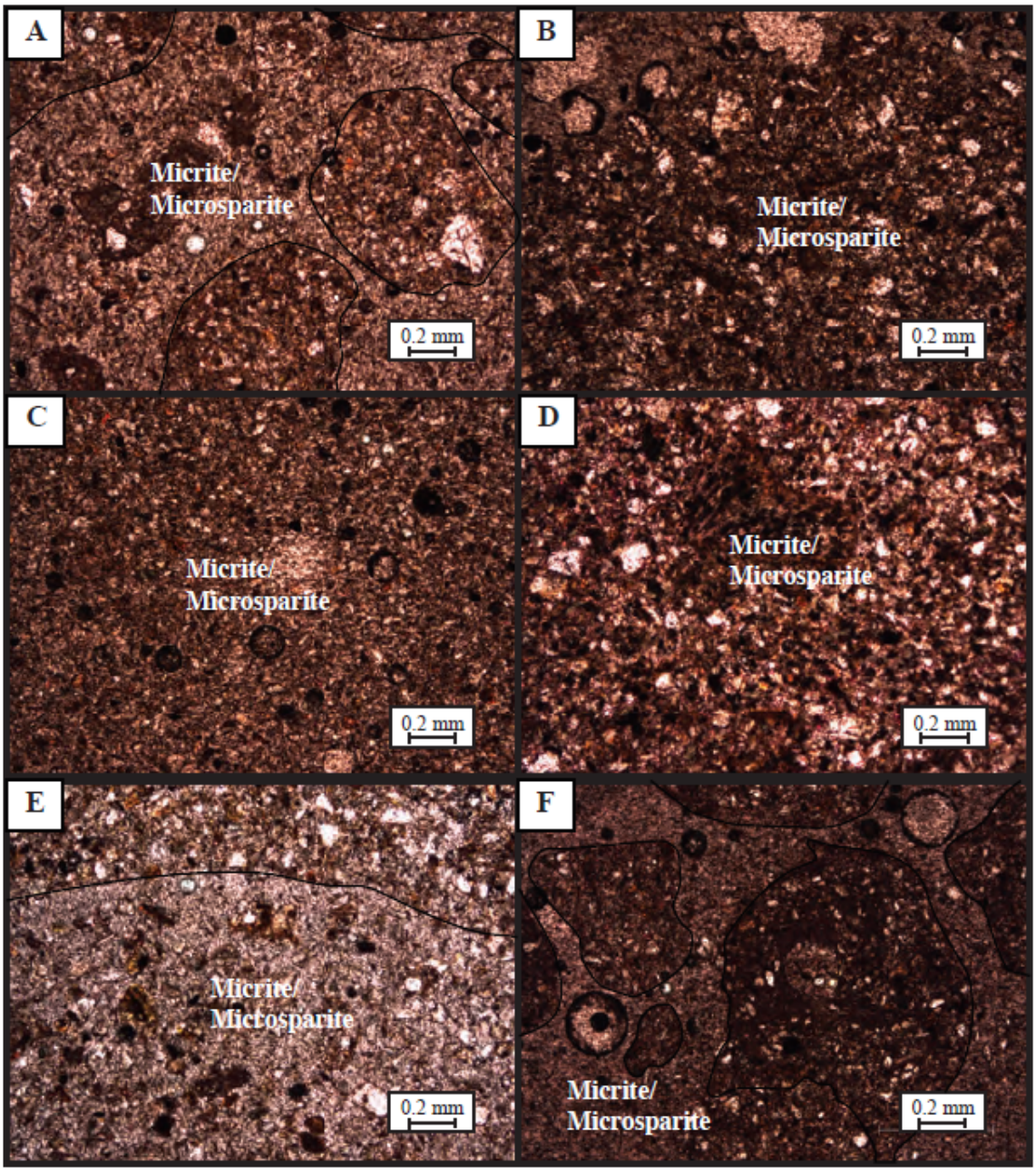

Figure S4. Examples of Washtucna paleosol thin sections in plane polarized light. Thin sections are carbonate stained with alizarin red-s and potassium ferricynide, and show the area containing micrite.

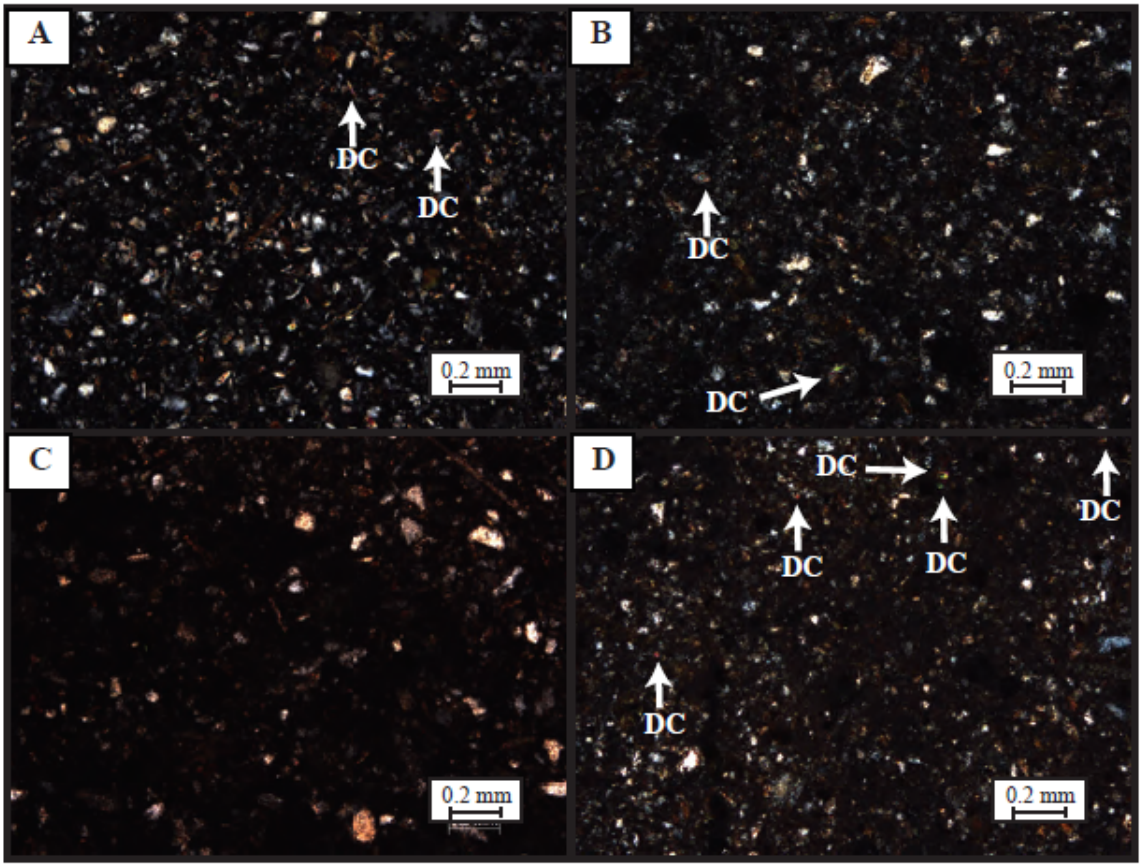

Figure S5. Examples of Sand Hills Coulee paleosol thin sections in cross-polarized light. White arrows are pointing to detrital carbonate (DC) giving second and third order red, blues and yellows.

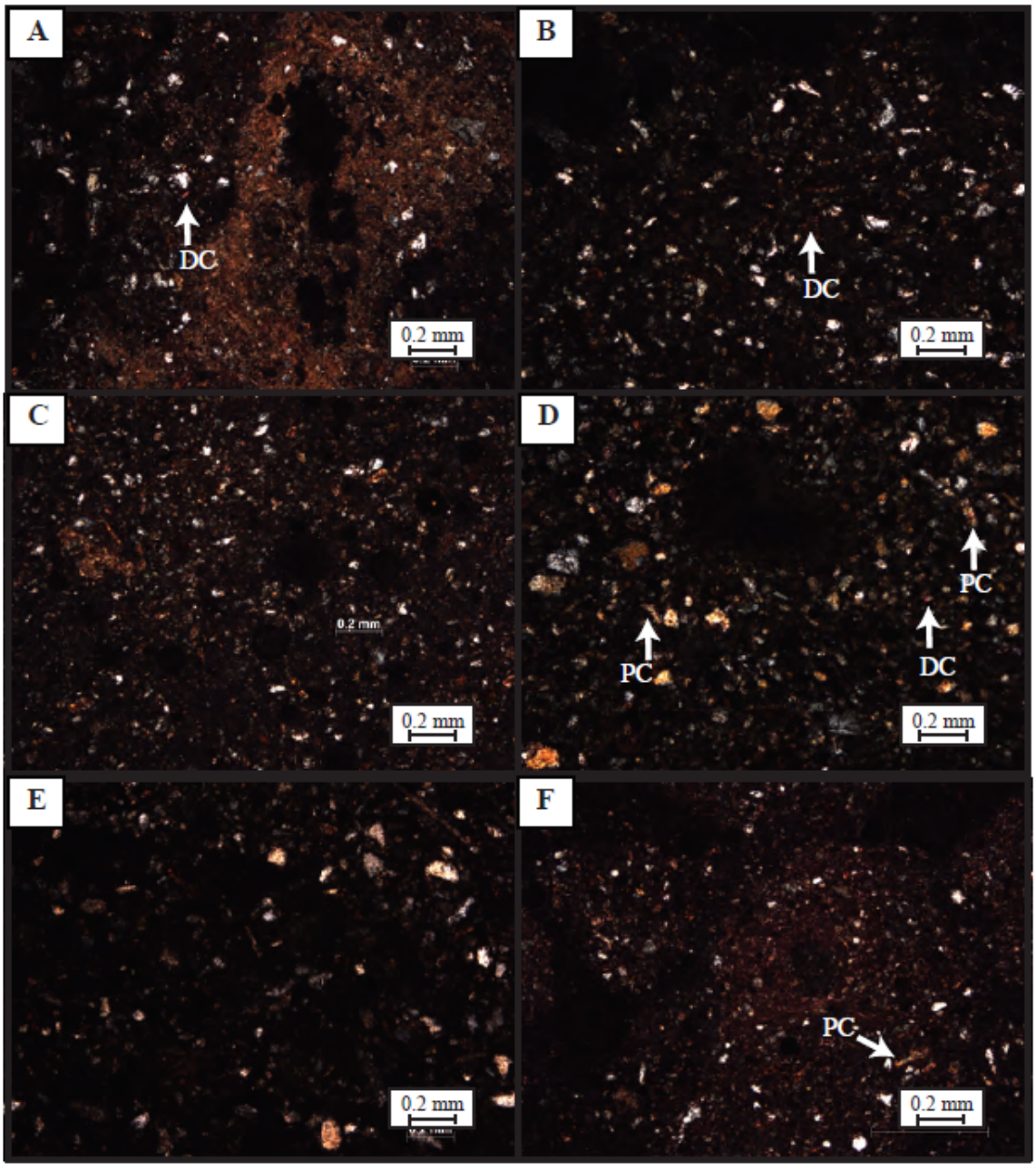

Figure S6. Examples of Washtucna paleosol thin sections in cross-polarized light. White arrows are pointing to detrital limestone or marble (DC) or pedogenic carbonate coatings (PC) within and around a mineral grain in second and third order red, blues, and yellows.

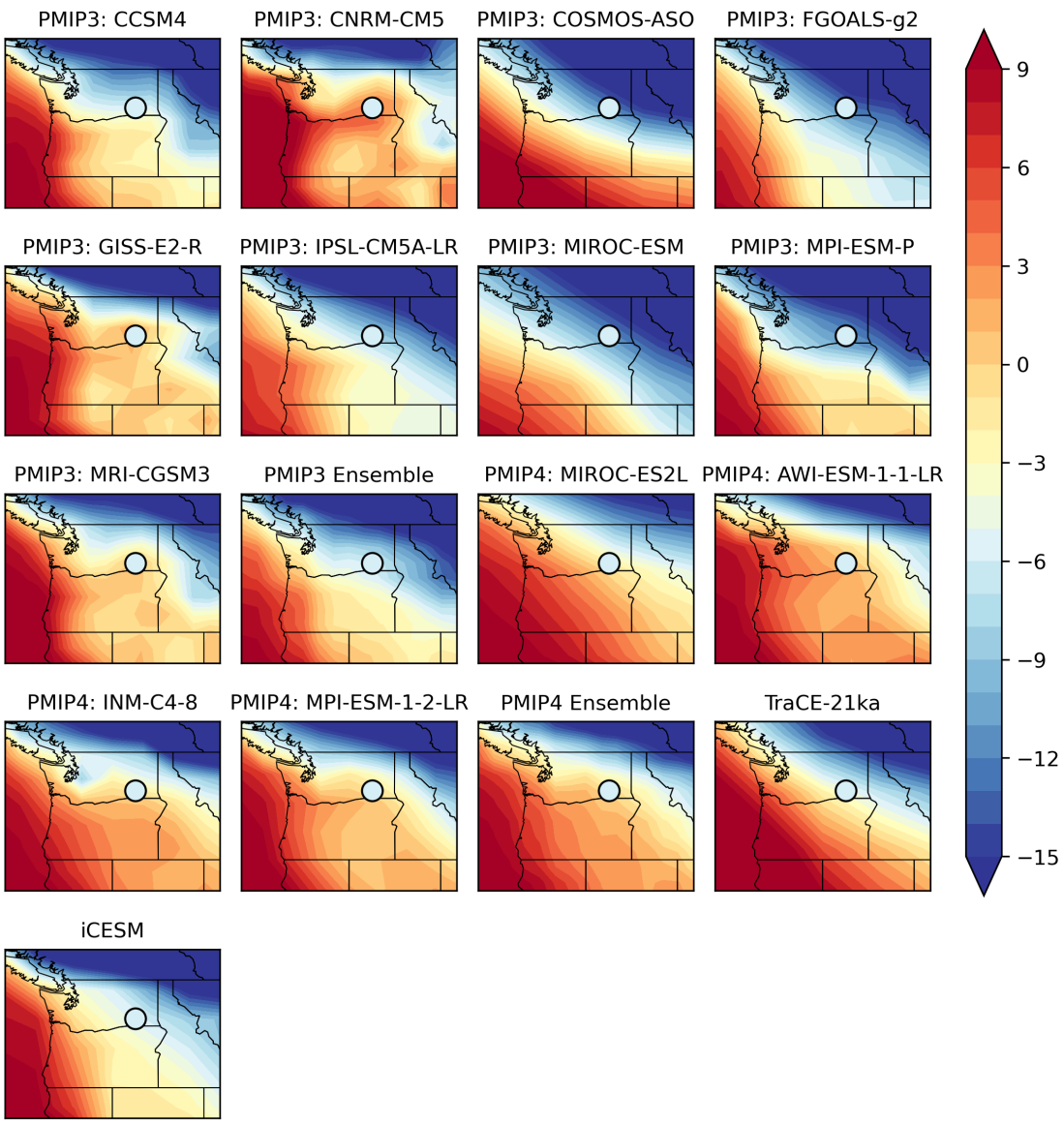

Figure S7: LGM temperatures for available models (PMIP3, PMIP4, TraCE-21ka, iCESM) compared to clumped isotope (circle; this work).

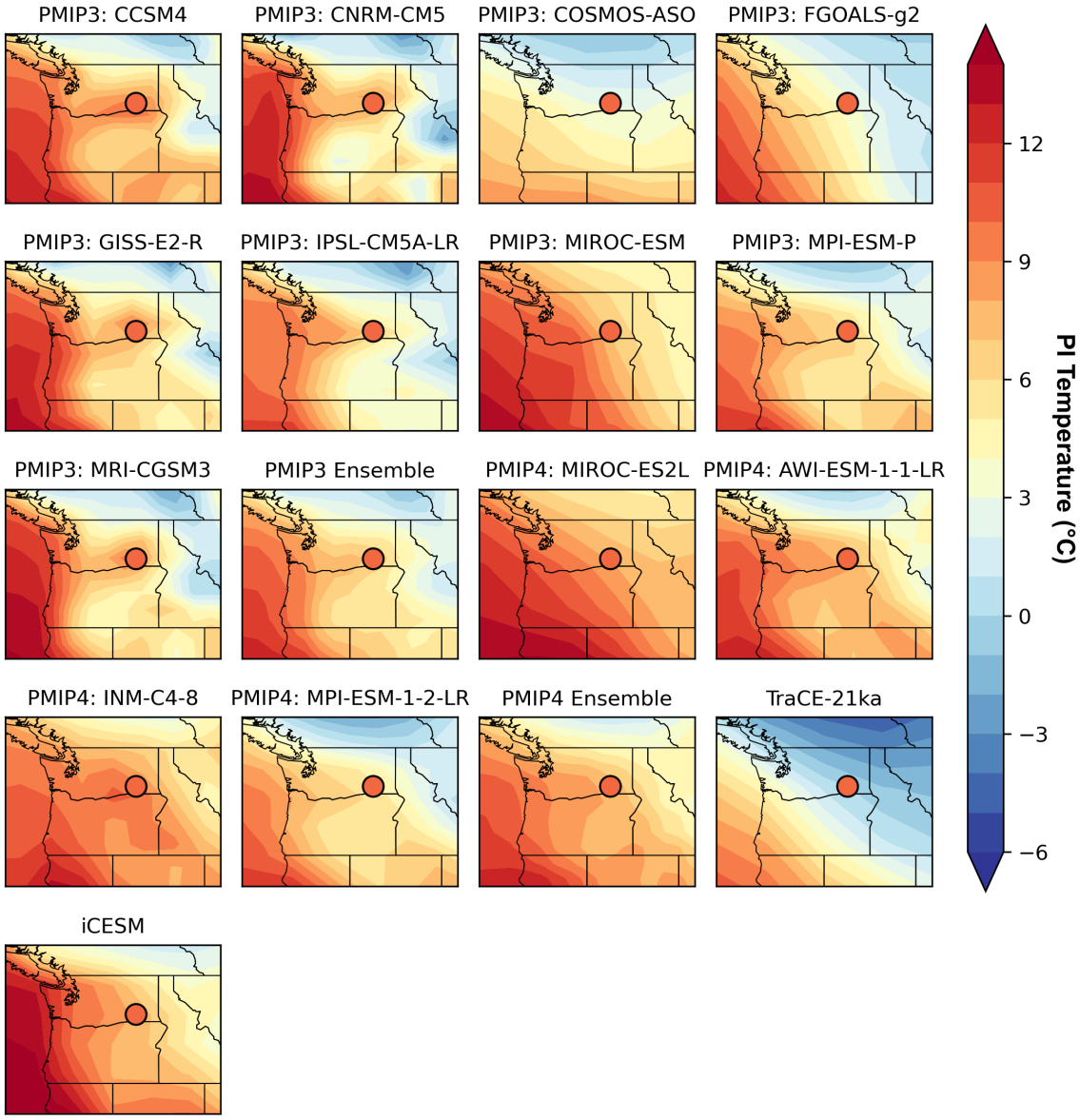

Figure S8: Pre-industrial temperatures for available models (PMIP3, PMIP4, TraCE-21ka, iCESM) compared to modern values (PRISM Climate Group, 2018).

Supporting Tables are also in a separate excel file.

Table S1. Mg/Ca and Mn/Ca Ratios of Bulk Carbonate.

Sample I.D.	Sample Type	Horizon	Bulk Carbonate Major Elements			Bulk Carbonate Ratios	
			Ca (mmol)	Mg (mmol)	Mn (micro mol)	Mg/Ca (mol/mol)	Mn/Ca (mmol/mol)
AY-1							
AY1SHC	Micritic Carbonate	Bkb1	0.29 +/– 0.01	0.02 +/– 0.00	0.04 +/– 0.00	0.05 +/– 0.03	0.13 +/– 0.03
AY1W3B	Micritic Carbonate/Carbonate Seam	Bkqmb2	0.73 +/– 0.01	0.02 +/– 0.00	0.02 +/– 0.00	0.02 +/– 0.01	0.03 +/– 0.01
AY1W3C	Micritic Carbonate	Bkqb2	0.09 +/– 0.00	0.02 +/– 0.00	0.02 +/– 0.00	0.16 +/– 0.01	0.22 +/– 0.01
AY1W3D	Micritic Carbonate/Carbonate Seam	Bkqmb2/Bkqb2	0.29 +/– 0.00	0.02 +/– 0.00	0.02 +/– 0.00	0.06 +/– 0.01	0.07 +/– 0.00
AY-2							
AY2SHC	Micritic Carbonate	Bkb1	0.25 +/– 0.00	0.01 +/– 0.00	0.01 +/– 0.00	0.06 +/– 0.02	0.03 +/– 0.01
AY2W3B	Micritic Carbonate	Bkqb2	0.29 +/– 0.01	0.02 +/– 0.00	0.01 +/– 0.00	0.05 +/– 0.04	0.04 +/– 0.03
AY2W3C	Micritic Carbonate/Carbonate Seam	Bkqmb2	0.34 +/– 0.00	0.02 +/– 0.00	0.01 +/– 0.00	0.05 +/– 0.01	0.03 +/– 0.01
WA-3							
WA3SHC	Micritic Carbonate	Bkb1	0.37 +/– 0.01	0.02 +/– 0.00	0.01 +/– 0.00	0.05 +/– 0.03	0.04 +/– 0.03
WA3W	Micritic Carbonate/Carbonate Seam	Bkqmb2	0.34 +/– 0.01	0.02 +/– 0.00	0.01 +/– 0.00	0.06 +/– 0.02	0.03 +/– 0.01
KP-1							
KP1SHC	Micritic Carbonate	Bkb1	0.29 +/– 0.01	0.01 +/– 0.00	0.04 +/– 0.00	0.04 +/– 0.02	0.15 +/– 0.02
KP1W	Micritic Carbonate	Bwb2	0.31 +/– 0.01	0.01 +/– 0.00	0.01 +/– 0.00	0.04 +/– 0.02	0.03 +/– 0.02

Table S2: Age Constraints. TL = thermoluminescence; ^{14}C AMS = radiocarbon

Site	Unit	Material Dated	Age Estimate (ka)	Uncertainty	Method	Stratigraphic Context	Source
KP-1	Sand Hills Coulee	Loess	14.0	+/- 2.4	TL	Straddling above MSH S tephra, slightly above Berger and Busacca, 1995.	Richardson et al., 1997.
KP-1	Sand Hills Coulee	Loess	17.0	+/- 2.8	TL	Straddling above MSH S tephra.	Berger and Busacca, 1995.
CHR-1	Sand Hills Coulee	Loess	8.2	+/- 1.6	TL	Located 77 cm above the cap of the Washtucna soil.	Blinnikov et al., 2002.
McFeely	Sand Hills Coulee	Gastropod	12.48	+/- 0.06	14 C AMS	Above MSH S tephra and below Glacier Peak Tephra (lengths are not provided by the authors).	Spencer and Knapp., 2010.
KP-1	Washtucna	Loess	20.4	+/- 1.4	TL	Straddling below MSH S tephra.	Berger and Busacca, 1995.
KP-1	Washtucna	Loess	17.2	+/- 1.9	TL	Straddling below MSH S tephra, slightly above Berger and Busacca, 1995.	Richardson et al., 1999.
CON-1	Washtucna	Loess	20.5	+/- 1.8	TL	Straddling below MSH S tephra.	Berger and Busacca, 1995.
CHR-1	Washtucna	Loess	33.2	+/- 3.4	TL	Located 58 cm below the base of the Sand Hills Coulee.	Richardson et al., 1999.
CLY-2	Washtucna	Loess	23.7	+/- 2.0	TL	Located approximately 160 cm below the MSH S Tephra.	Richardson et al., 1997.
CLY-2	Washtucna	Loess	36.1	+/- 4.3	TL	Located approximately 270 cm below the MSH S Tephra.	Richardson et al., 1997.
CLY-2	Washtucna	Loess	40.1	+/- 3.7	TL	Locted approximately 370 cm below the MSH S Tephra.	Richardson et al., 1997.
Marias Pass	Glacier Peak Tephra	Twig Fragments	11.6 Cal.	+/- 0.05	14 C AMS	Located below the cap of the Sand Hills Coulee soil.	Kuehn et al., 2009.
NA	MSH S Tephra	NA	15.4 Cal.	+/- 0.1	14 C AMS	Seperates the Sand Hills Coulee soil and Washtucna soil, overlain by L1 loess and underlain by L2 loess.	Richardson et al., 1997.

Table S3. Estimated Loess Sedimentation Rates

Site	Time Period	Estimated Loess Sedimention Rate	Source
KP-1	after 15 ka	>20 cm/k.y.	Sweeny et al., 2004
CLY-1	after 15 ka	>20 cm/k.y.	Sweeny et al., 2004
KP-1	35 - 15 ka	6 cm/k.y.	Sweeny et al., 2004
CLY-1	35 - 15 ka	6 cm/k.y.	Sweeny et al., 2004
KP-1	prior 35 ka	>20 cm/k.y.	Sweeny et al., 2004
CLY-1	prior 35 ka	>20 cm/k.y.	Sweeny et al., 2004

Table S4. Air Temperature Transfer Functions and modern climate data (monthly air temperatures from PRISM Climate Group, 2017, and modern carbonate formation temperatures from Takeuchi et al., 2009).

Air Temperature Interval	Equation	R^2	Source
Mean Annual	MAAT = 1.20*TC(D47) - 21.72	0.92	Quade et al., 2012
June-August	WAMT = 1.13*TC(D47) - 10.81	0.89	Quade et al., 2013

Month	Monthly Mean	MAT Modern	WAMT Modern	Carbonate Formation Temperatures
Jan	0.6	10.9	21.2	14.6 °C to 20.7 °C
Feb	2.8			
March	6.7			
Apr	10.3			
May	14.4			
Jun	18.3			
Jul	22.6			
Aug	22.6			
Sep	17.7			
Oct	11.1			
Nov	4.6			
Dec	-0.3			

Table S5: TraCE simulation results used for this work. TraCE simulations described in Liu et al. (2009). All data regridded and output to 46.5 ºN,118.5 ºW.

	Temperature (K)		Temperature (ºC)	
Time (ka)	**MAT**	**JJA**	**MAT**	**JJA**
22	266.6	276.7	-6.6	3.6
21	266.5	276.7	-6.7	3.6
20	266.6	277.3	-6.6	4.2
19	266.5	277.6	-6.7	4.5
18	266.7	278.3	-6.5	5.2
17	267.3	279.6	-5.9	6.5
16	268.5	281.7	-4.7	8.6
15	270	283.3	-3.2	10.2
14	271.5	284.5	-1.7	11.4
13	272.5	284.8	-0.7	11.7
12	272.9	284.5	-0.3	11.4
11	273.6	285.2	0.5	12.1
10	273.9	285.3	0.8	12.2
9	273.9	285.1	0.8	12.0
8	273.9	284.6	0.8	11.5
7	274.1	284.4	1.0	11.3
6	273.9	284	0.8	10.9
5	274	283.9	0.9	10.8
4	274	283.7	0.9	10.6
3	274	283.5	0.9	10.4
2	274	283.5	0.9	10.4
1	273.9	283.5	0.8	10.4
0	273.9	283.5	0.8	10.4

Table S6: Simulation results used for this work. PMIP3 simulations described in Braconnot et al. (2012). PMIP4 simulations described in Kageyama et al. (2021). TraCE simulations described in Liu et al. (2009). iCESM simulations described in Brady et al. (2019).

PMIP3 MODELS: (46.5 °N,118.5-°W)

Model	PI MAT (°C)	LGM MAT (°C)	Temperature Anomaly (°C)
CCSM4	9.1	-6.1	-15.2
CNRM-CM5	8.4	3.2	-5.1
COSMOS-ASO	3.1	-12.8	-15.9
FGOALS-g2	3.3	-11.7	-15.1
GISS-E2-R	9.5	2.1	-7.4
IPSL-CM5A-LR	7.9	-6.2	-14.1
MIROC-ESM	6.7	-10.9	-17.6
MPI-ESM-P	6.2	-10.3	-16.5
MRI-CGCM3	8.7	0.2	-8.5
PMIP3 Ensemble	7.0	-5.9	-12.9

PMIP4 MODELS: (46.5 °N,118.5 °W)

Model	PI MAT (°C)	LGM MAT (°C)	Temperature Anomaly (°C)
MIROC-ES2L	8.0	-1.1	-9.1
AWI-ESM-1-1-LR	7.9	1.7	-6.1
INM-CM4-8	9.8	0.8	-9.0
MPI-ESM-1-2-LR	5.6	0.5	-5.1
PMIP4 Ensemble	7.7	-0.4	-8.0

iCESM

PI MAT (°C)	LGM MAT (°C)	Temperature Anomaly (°C)	PI JJA(°C)	LGM JJA (°C)	Temperature Anomaly (°C)
7.0	-6.2	-13.2	18.4	9.6	8.8

TraCE

PI MAT (°C)	LGM MAT (°C)	Temperature Anomaly (°C)	PI JJA(°C)	LGM JJA (°C)	Temperature Anomaly (°C)
0.8	-6.6	-7.4	10.4	3.6	6.8

Table S7: Stable isotope data for samples and standards.

Sample	**N**	**$\delta^{13}C$ Average (VPDB, ‰)**	**1 s.d.**	**1 s.e.**	**$\delta^{18}O$ Average (VPDB, ‰)**	**1 s.d.**	**1 s.e.**	**Δ_{47} Average (I-CDES, ‰)**	**1 s.d.**	**1 s.e.**
Carmel Chalk	75	-2.2	0.1	0.0	-3.9	0.1	0.0	0.594	0.018	0.002
Carrara Marble	69	2.1	0.1	0.0	-1.5	0.1	0.0	0.312	0.021	0.003

CMTile	14	2.0	0.0	0.0	-1.5	0.1	0.0	0.313	0.017	0.005
ETH-1	54	2.0	0.1	0.0	-2.2	0.1	0.0	0.205	0.020	0.003
ETH-2	51	-10.2	0.1	0.0	-18.7	0.1	0.0	0.207	0.024	0.003
ETH-3	54	1.7	0.1	0.0	-1.8	0.1	0.0	0.613	0.021	0.003
ETH-4	49	-10.2	0.0	0.0	-18.8	0.1	0.0	0.442	0.021	0.003
Mallinckrodt	7	-40.3	0.1	0.0	-21.9	0.1	0.0	0.463	0.027	0.010
NBS 19	7	1.9	0.0	0.0	-2.1	0.1	0.0	0.326	0.043	0.016
SRM 88B	2	2.0	0.1	0.1	-7.6	0.0	0.0	0.514	0.001	0.001
TV03	29	2.6	0.1	0.0	-8.3	0.1	0.0	0.625	0.022	0.004
Veinstrom	67	-6.2	0.1	0.0	-12.6	0.1	0.0	0.632	0.018	0.002
Bonedry Tank CO2	122	-	-	-	-	-	-	1000°C equilibration (stochastic)		
Evap DI + Carrera Marble CO2		-	-	-	-	-	-	1000°C equilibration (stochastic)		
Bonedry Tank CO2	148	-	-	-	-	-	-	25°C equilibration		
Evap DI + Carrera Marble CO2		-	-	-	-	-	-	25°C equilibration		